ELSEVIER

Biochimica et Biophysica Acta 1375 (1998) 117–130

BIOCHIMICA ET BIOPHYSICA ACTA
BBA

A Ca^{2+}- and voltage-dependent cation channel in the nuclear envelope of red beet

Czeslawa Grygorczyk, Ryszard Grygorczyk *

Department of Biology, McGill University, 1205 Doctor Penfield Ave., Montréal, Que. H3A 1B1, Canada

Received 22 June 1998; accepted 10 August 1998

Abstract

The patch-clamp technique was applied to study ion conductances in various configurations of the nuclear envelope of non-enzyme-treated red beet (*Beta vulgaris* L.) nuclei. With excised patches a non-selective cation channel was observed, that was activated by micromolar concentrations of Ca^{2+} on the nucleoplasmic side of the envelope. The channel activity was also voltage-dependent and the voltage threshold of channel activation changed with the nucleoplasmic Ca^{2+} concentration. The most prominent conductance level was 110 ± 22 pS with 150 mM KCl in the bath and pipette. The channel was permeable to small cations: permeabilities relative to K^+ were $P_K \cong P_{Na} = 1$, $P_{Cs} = 0.3$, but $P_{Cl} = 0.09$. Calcium ions also permeated the channel with $P_{Ca} = 0.43$, estimated from reversal potential, or 0.14, estimated from conductance ratio. Zn^{2+} (1 mM) when applied to the cytoplasmic side of the envelope blocked the channel activity completely, while amiloride (2 mM) reduced the channel current by 86% from the nucleoplasmic side. The properties of the whole-nucleus current (voltage-, time- and Ca^{2+}-dependence) paralleled those observed with excised patches. The channel may provide a Ca^{2+}-regulated pathway for passive diffusion of cations across the nuclear envelope and thus may play an important role in Ca^{2+}-dependent nuclear processes ranging from gene transcription to apoptosis.

Keywords: Nuclear envelope; Ion channel; Cation channel; (*Beta vulgaris*)

1. Introduction

The nuclear envelope (NE) of eukaryotic cells separates the genome from the cytoplasm. It consists of two concentric bilayers that are perforated and held together by nuclear pore complexes (NPC). Electrophysiological studies have revealed several types of ion channels that are present in the nuclear envelope (for review see [1–4]). Two types of chloride channels as well as a cation-selective channels have been found following fractionation and reconstitution of inner and outer membrane fractions of sheep cardiac nuclei into lipid bilayers [5]. A nuclear chloride ion channel was recently cloned from the human myelomonocytic cell line [6]. In addition to ion channels that presumably reside either in the inner or outer membrane of the NE [5,7], several studies indicate the existence of ion channels traversing both membranes of the NE, e.g. in cardiac myocytes [8] and avian erythrocytes [9], thus providing a direct pathway for ion flow between nucleoplasm and cyto-

Abbreviations: NE, nuclear envelope; NPC, nuclear pore complex; DAPI, 4′,6′-diamidino-2-phenylindole; V_{LJ}, liquid junction potential

* Corresponding author. Present address: Centre de Recherche Hôtel Dieu de Montréal, 3850 rue Saint-Urbain, Montréal, Que. H2W 1T8, Canada.
E-mail: grygorcr@magellan.umontreal.ca

0005-2736/98/$ – see front matter
PII: S0005-2736(98)00142-4

plasm. It is suggested that these ion channels may be associated with or be a part of the NPC [10].

Little is known about the roles of the various NE ion channels and their regulation, e.g. by Ca^{2+} ions, although Ca^{2+} and Ca^{2+}-binding proteins play important roles, not only in cytoplasmic signal transduction, but also in a variety of nuclear processes including gene expression, DNA replication and DNA repair [11–16]. Inositol trisphosphate (IP_3) receptor channels, selective for calcium and inhibited by heparin, have been found for example in *Xenopus* oocyte nuclei [13,14,17,18]. Recent findings indicate that passive diffusion of intermediate-sized molecules (relative molecular mass of approximately 10 000) between nucleoplasm and the cytosol may be regulated by the conformational state of the NPC and that depletion of perinuclear Ca^{2+} stores inhibits this diffusion process [12]. Altogether, these data strongly suggests that the NE represents an autonomous system controlling Ca^{2+} homeostasis in the nucleus and thus Ca^{2+}-dependent nuclear processes. Here we report the presence of a cation-selective, Ca^{2+}- and voltage-dependent channel in the membrane of the red beet NE. The channel provides a Ca^{2+}-regulated pathway for cation flow across NE membranes and may therefore be involved in the regulation of Ca^{2+}-dependent nuclear events.

Preliminary results of this study have been published in abstract form [19].

2. Materials and methods

2.1. Solutions

All chemicals used were of analytical grade. The standard solution used in the bath and pipette if not stated otherwise, contained (in mM): 150 KCl, 2 $MgCl_2$, 10 *N*-2-hydroxyethylpiperazine-*N*′-2-ethanesulfonic acid (HEPES), 100 sorbitol and was buffered with Tris or KOH to pH 7.2. The contaminating Ca^{2+} concentration in this solution was approximately 5 μM as estimated by flame absorption analysis. In some experiments desired free Ca^{2+} concentrations were obtained by mixing at different ratios K_2Ca-ethylene glycol-bis(b-aminoethyl ether *N*,*N*,*N*′,*N*′-tetraacetic acid (K_2Ca-EGTA) and K_2H_2-EGTA. Stocks (1 M) of K_2Ca-EGTA and K_2H_2-EGTA were prepared by pH metric method of Moisescu and Pusch and titrated to pH 7.2 as described by Tsien and Pozzan [20]. The Ca^{2+} concentrations were calculated using a computer program that corrects the association constants for temperature, pH and ionic strength [21]. For Ca^{2+} concentrations of 0.1 mM and higher EGTA was omitted and $CaCl_2$ added as required. The osmolarity of the media was adjusted with sorbitol to 420 ± 10 mOsm/kg H_2O as measured with a vapor pressure osmometer, Wescor 5500 (Wescor, Logan, UT, USA).

For experiments where selectivity of the channel was studied, K^+ in the above solution was replaced by Na^+ or Cs^+. Other solutions are described in the text.

2.2. Isolation and identification of nuclei

For the patch-clamp experiments about 1 μl of juice from freshly scraped storage tissue of red beet (*Beta vulgaris* L.) was deposited on the bottom of the recording chamber containing approximately 1 ml of the standard 150 mM KCl solution. Several vacuoles and nuclei could easily be found in the juice as a result of mechanical cell disruption. Debris was washed out by gentle perfusion, leaving nuclei attached to the glass bottom of the recording chamber.

For the purpose of identification of nuclei using fluorescence microscopy, red beet protoplasts were isolated enzymatically as follows: approximately 1 g of red beet tissue was cut into small pieces (1–2 mm) using a razor blade and treated with 10 ml of enzyme solution for about 30 min at 27°C, pH 6.0, 870 mOsm/kg H_2O. The enzyme solution contained: 23.25 g/l Gamborg basal salt mixture (Sigma, B-5), 10 mM 2-(*N*-morpholino)ethanesulfonic acid (MES), 2 mM dithiothreitol, 1.5% Cellulase Y-C, 0.5% Macerozyme R-10, 0.5% Pectolyase Y-23, 0.5% bovine serum albumin, 60 g/l mannitol. Before use, the enzyme solution was filtered through a 0.2 mm filter (Millipore).

For the electron microscopy thin slices of red beet tissue were fixed with 2.5% glutaraldehyde buffered with 0.1 M sodium phosphate and postfixed with 1% osmium tetroxide in 0.1 M sodium phosphate. They were dehydrated in graded series of ethanol solutions and embedded in EPON. Ultrathin sections were

stained with uranyl acetate followed by lead citrate treatment. The preparations were examined at different magnifications with a Philips EM410 electron microscope, operated at 80 keV.

2.3. Electrophysiology

Standard patch-clamp technique [22] was utilized throughout the study. Patch pipettes were pulled in two stages (Narishige PP-82 puller) from borosilicate glass capillaries (0.35 mm wall thickness, 6285, A-M Systems, Everett, WA) and had a resistance of 5–15 MΩ when filled with 150 mM KCl. Ion currents were recorded using a List EP-7 patch-clamp amplifier (List Medical, Darmstadt, Germany). Currents were low-pass filtered at 10 kHz and recorded on VCR tape through a pulse-code modulator (PCM2, Medical Systems Greenvale, NY, USA). For voltage-jump experiments, a LABMASTER TL-1 DMA interface and pCLAMP software (version 5.5, Axon Instruments, Foster City, CA) were used to generate waveforms, acquire and analyze the data. In experiments performed in whole-nucleus configuration, the nucleus capacitance was compensated using analog circuitry within the patch-clamp amplifier.

Liquid junction potentials V_{LJ} were measured as described by Neher [23] and their polarity follows the convention of Barry, i.e. V_{LJ} is defined as the potential of the bath solution with respect to pipette solution [23]. For all our experimental conditions, except experiments with 50 mM $CaCl_2$, V_{LJ} were found to be less than 1 mV and were neglected. In experiments with 50 mM $CaCl_2$ in the bath and 150 KCl in pipette, $V_{LJ} = +5.2$ mV, and was used to correct the current reversal potential for calculation of Ca^{2+} permeability.

All experiments were performed at room temperature, 22–25°C.

2.4. Sign convention

Voltages across the patch of the nuclear envelope refer to the nucleoplasmic side of the patch with respect to the cytoplasmic side. Thus, positive voltage corresponds to positive on the nucleoplasmic side; positive current means current flowing from nucleus to cytoplasm and is shown in the figures as upward deflection.

2.5. Seal formation and membrane configurations

In approximately 50% of attempts, gigaohm seals (5–20 GΩ) were obtained on the nuclei upon application of slight suction of less than 10 mmHg to the patch pipette. Brief exposure to air of the nucleus sealed to the pipette led to formation of an excised, inside-out patch of the NE. By applying a pulse of suction in nucleus-attached mode, to break the patch under the pipette, a whole-nucleus-like configuration could be established. Experiments with pipette solutions containing 10 μM fluorescein-labeled dextran (70 kDa, Molecular Probes, Eugene, OR) which has been found not to penetrate intact nuclei, at least those not damaged during isolation [24], showed a fluorescence pattern consistent with dextran diffusion not restricted to the perinuclear space, but rather distributed homogeneously in the bulk of the nucleus (not shown).

On a few occasions, after formation of the whole-nucleus configuration, withdrawal of the pipette from the nucleus led to the formation of an excised outside-out patch, as indicated by the sidedness of the effect of voltage on channel activity (see Section 3). In the present study, 34 experiments were performed with excised inside-out patches of the NE, three with excised outside-out patches and 21 experiments in whole-nucleus configuration.

3. Results

3.1. Identification and morphology of the red beet nucleus

In enzymatically isolated, intact red beet protoplasts, the nucleus can be seen by conventional light microscopy as an ellipsoid or spherical object of 8–20 μm in diameter within the cytoplasm, while the vacuole, which typically occupies most of the cell volume, is seen as a dark sphere (Fig. 1A). When treated with the DNA-selective stain DAPI, the nucleus is seen as a bright object under fluorescence microscopy (Fig. 1B). Electron micrographs (see Fig. 2 below), confirmed that such objects possess a double membrane, typical of nuclear envelope. On several occasions, we have observed nuclei 'popping out' of the enzymatically treated protoplasts. A sim-

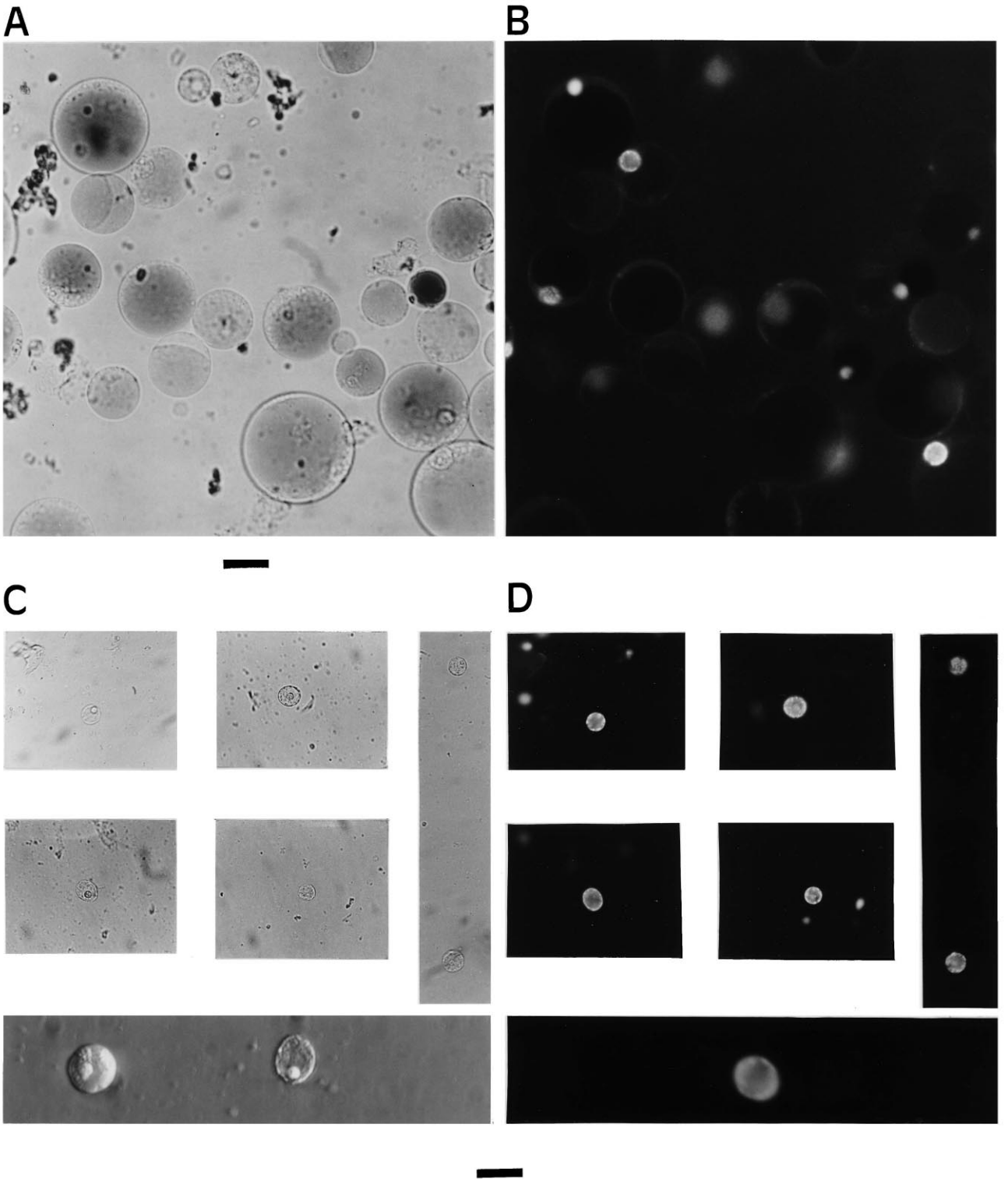

ilar phenomenon was reported previously for enzymatically isolated protoplasts of *Allium cepa* [25]. Isolated nuclei can also be found in a red beet juice and were indistinguishable from those that popped

Fig. 1. Identification and morphological properties of the red beet nucleus. (A) Enzymatically isolated red beet protoplasts seen by conventional light microscopy. (B) The same protoplasts treated with the DNA-selective stain DAPI under fluorescence microscopy. The DAPI-stained nuclei are clearly seen as bright spherical objects. (C) Isolated nuclei found in the juice of the red beet observed under conventional light microscopy. Due to low number of nuclei in a juice, sections from different fields of view are shown. The bottom section shows two nuclei at higher magnification. (D) The same nuclei as in C seen under fluorescence microscopy using DAPI staining, except the bottom section. The bottom sections in C and D are from different fields of view due to use of different films (see below). The scaling bar corresponds to 30 μm for all photographs except bottom section in C and D where it corresponds to 15 μm. The photographs were made on an inverted microscope used for patch-clamp experiments (Fluoreszenz Leica DM-IL, Leitz Wetzlar Germany) equipped with oil immersion objective NPL Fluotar 25/0.75 NA oil, (400 ASA film). The bottom section in C was made using Hoffman Modulation Contrast objective 40×LWD/HMC/0.50 NA (100 ASA film) and the bottom section in D was made with FL 40/1.3 NA oil immersion objective (400 ASA film).
←

out of the protoplast. All showed the same morphological features (shape, size, presence of nucleoli) as well as specific labeling by DAPI like those in intact protoplasts (Fig. 1C,D). The isolated nuclei were also specifically stained with ethidium bromide (not shown). Later, in electrophysiological experiments, use of DNA stains was avoided and nuclei were identified only by their morphological features. Also all experiments described below were performed on nuclei originating from the red beet juice, thus the use of any enzymes for isolation of nuclei was avoided.

Since NE is continuous with the endoplasmic reticulum (ER), NE patches studied here could actually contain some membrane that originated from the ER. However, electron micrographs of red beet tissue slices shown in Fig. 2 confirmed a previous report [26] that there is very little endoplasmic reticulum membrane present, which therefore should make a negligible contribution to the NE membrane patches studied by electrophysiology.

3.2. Recordings with excised patches of nuclear envelope

Most nucleus-attached patches (95%) of the NE were quiescent. However, excision of the patch (inside-out configuration) resulted in immediate activation of ion channels when the bathing medium contained free Ca^{2+} at a concentration above 0.1 μM. After excision, virtually all patches showed the presence of several tens and in some cases more then a hundred of active channels, suggesting their high density. Channel activity was abolished when inside-out patches were perfused with bathing solution containing 0 $CaCl_2$ and 1 mM EGTA (Fig. 3A). Channel activity also showed profound voltage-dependence: with 1 μM free Ca^{2+} and holding potentials negative to −20 mV on the nucleoplasmic side of the patch, no channel openings were observed. The channel activity increased dramatically when the patch was held at potentials positive to +10 mV (Fig. 3B). This voltage and Ca^{2+} dependence was studied in more detail in experiments such as the one illustrated in Fig. 3C. The nucleoplasmic face of the inside-out patch of the NE was perfused with bathing solution containing different concentrations of free Ca^{2+} buffered with 10 mM EGTA. At each Ca^{2+} concentration, the patch was subjected to the sequence of voltage steps and the corresponding current responses were recorded. With no Ca^{2+} added (panel labeled 0 in Fig. 3C), no channel openings were observed in the whole voltage range tested (from −120 to +120 mV). When the bathing solution contained 0.16 μM Ca^{2+} single-channel openings were observed only at voltages positive to +40 mV. Increasing the concentration of free Ca^{2+} to 1.4 or 5 μM activated large outward currents, two lower panels in Fig. 3C. These currents resulted from opening of a large number of individual channels, approximately 180 channels in this patch. The individual channels could be resolved using tail current analysis as described below. Fig. 3D summarises the voltage dependence of channel activity expressed as open state probability P_o for N channels in the patch, NP_o, at different free Ca^{2+} concentrations tested in this experiment. At 1.4 μM the NP_o-voltage dependence was sigmoidal and shifted to the left compared to 0.16 μM free Ca^{2+}. Higher Ca^{2+} concentrations of 5 and 13.9 μM resulted in saturating activity of the channel for voltages positive to +20 mV. In addition to voltage-dependence, a time-dependent channel activation was observed during the voltage steps and is

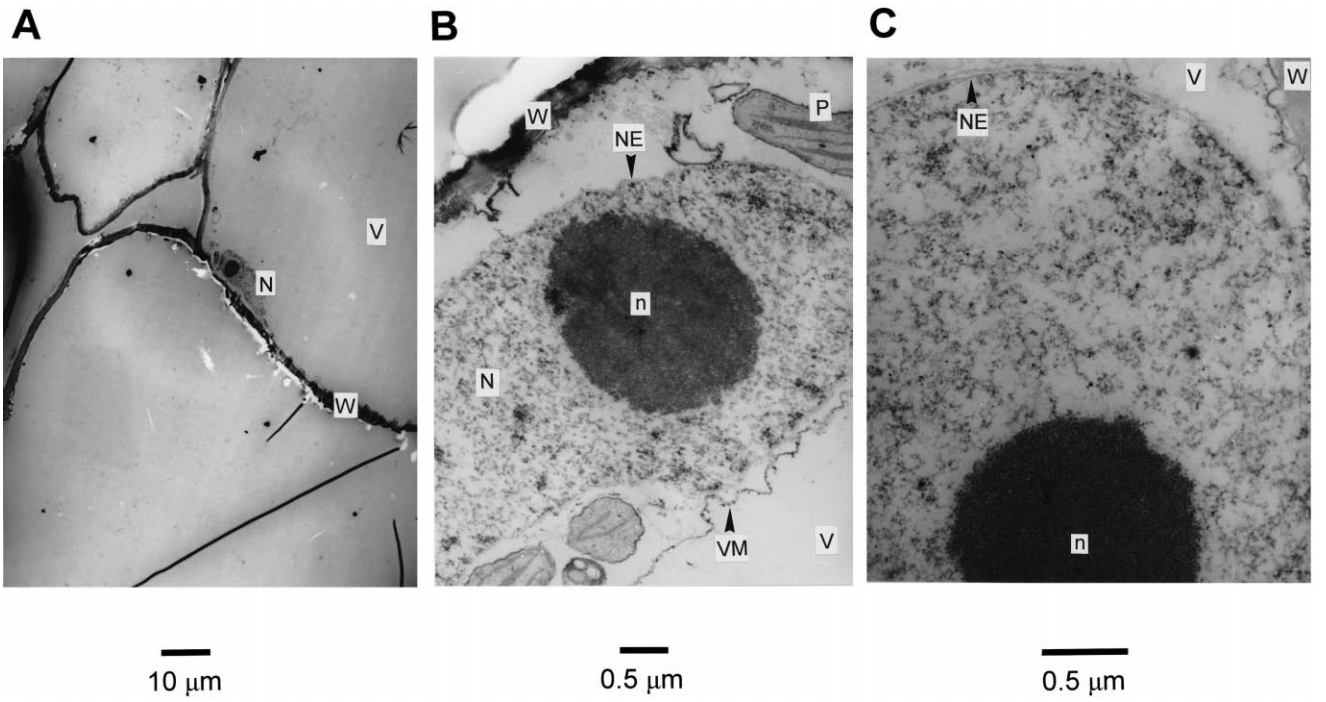

Fig. 2. Examples of electron micrographs of red beet tissue slices. The relatively small size of the nucleus, typically located at the cell wall, compared to the space occupied by the vacuole is shown in A. Plastids and vacuolar membrane are clearly seen in B; the two membranes of the NE could be distinguished in C. Very little endoplasmic reticulum membranes could be found in all electron micrographs examined. N, nucleus; n, nucleolus; NE, nuclear envelope; V, vacuole; VM, vacuolar membrane; P, plastid; W, cell wall.

illustrated in Fig. 4A. The channel openings were seen only at positive potentials on the nucleoplasmic side of the NE patch. It can also be seen that the channel activity showed sigmoidal time-dependence: at the onset of a depolarizing pulse (e.g. +60 mV), all channels were closed, but they opened in increasing numbers until their activity reached a steady state at the end of the 500 ms pulse. The sigmoidal time-dependence of channel activation is better illustrated in Fig. 4B, which shows the mean of 13 current traces from the same patch in response to repetitive stimulation by a +60 mV voltage step. Because of this voltage- and time-dependence, in order to construct the current–voltage relation (*I–V*) in the full voltage range we have used a two-pulse voltage protocol (Fig. 4C). Here the channels were activated by a 500 ms prepulse of +60 mV and then a test pulse was applied. The channels opened by the depolarizing prepulse deactivated quickly when potential was stepped to negative values, which was seen as a stepwise decrease of the tail current. The *I–V* relation obtained from the current steps within the tail current is shown in Fig. 4D, and in this experiment it has a slope conductance of 112 pS. Similar channels were observed in other excised patch experiments and their conductance was (mean ± S.D.) 110 ± 22 pS ($n = 24$).

The channel activity in inside out patches was blocked completely by 1 mM Zn^{2+} added to the bath ($n = 3$), while nucleoplasmic amiloride (2 mM) reversibly reduced macroscopic patch current by 86 ± 5% in the voltage range of +20 to +120 mV ($n = 2$, not shown).

3.3. Selectivity of the channel

In order to determine channel selectivity, shifts of the reversal potential of the single-channel currents were studied under various ionic conditions. With the pipette containing 50 mM KCl and the bath 300 mM KCl, the single-channel *I–V* reversal potential was shifted by approximately −35 ± 2 mV ($n = 3$). An example of such an experiment is shown in Fig. 5A, which demonstrates that the channel was preferentially selective for cations over anions. Different slope conductances below and above the reversal po-

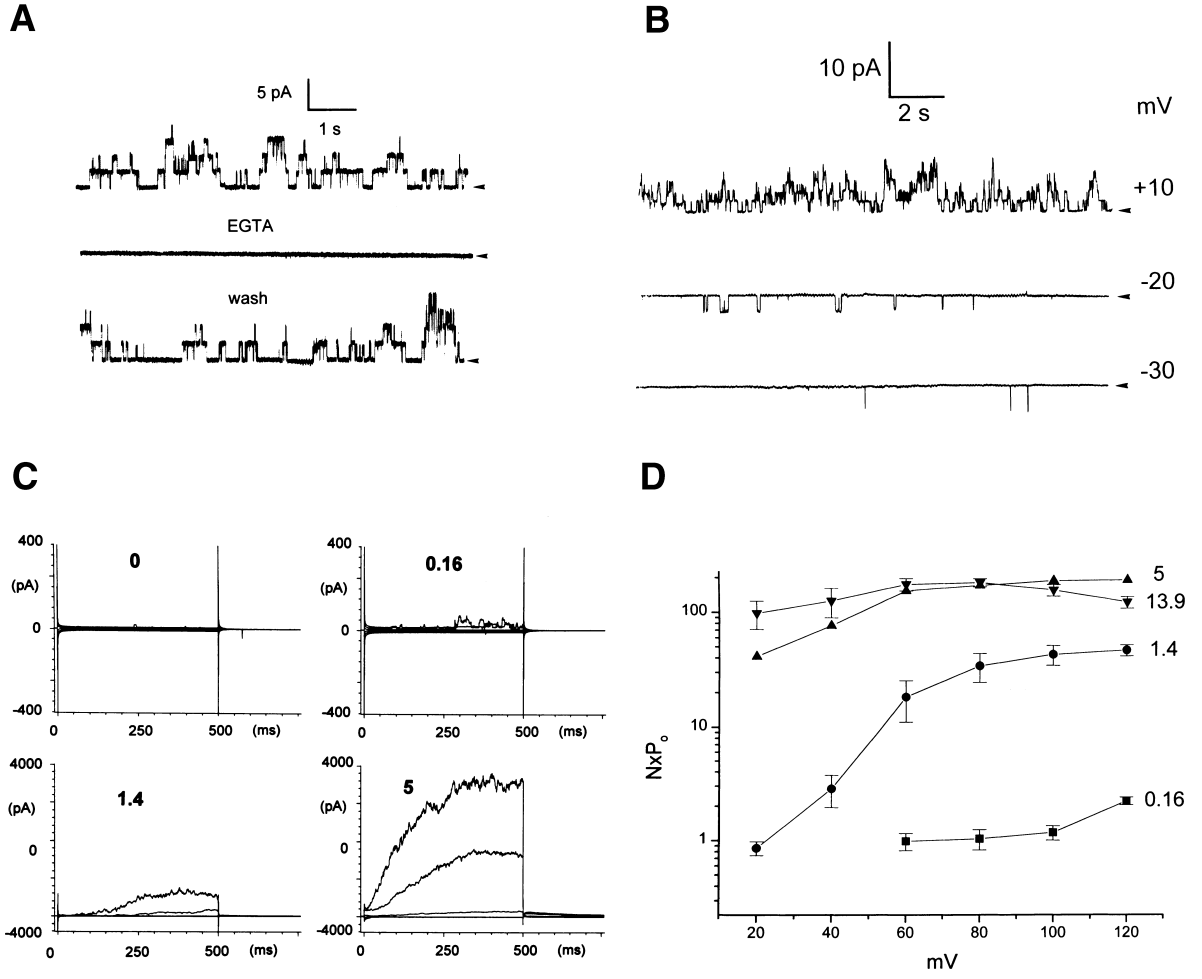

Fig. 3. Channel activity is Ca^{2+} and voltage-dependent. (A) Example of an experiment demonstrating regulation of channel activity by Ca^{2+}. Upper trace shows current fluctuations observed with an excised inside-out patch of the nuclear envelope with the pipette and the bath media containing the standard 150 mM KCl solution and 0.1 mM $CaCl_2$. Channel activity was completely abolished when the bath was perfused with Ca^{2+}-free media containing 1 mM EGTA (middle trace), and the effect was reversed upon wash with media containing 0.1 mM Ca^{2+} and 0 EGTA (lower trace). The effect could be reproduced several times with the same membrane patch (not shown). The patch was held at +20 mV; arrowheads indicate current baseline and upward deflections of the current trace correspond to channel open state, i.e. to current flow out of the nucleus. (B) Activity of the channel is voltage dependent. Current fluctuations observed in symmetrical 150 mM KCl solutions with an excised inside-out patch of the nuclear envelope at different holding voltages shown on the figure. Solution bathing the nucleoplasmic side of the patch contained 1 μM free Ca^{2+} buffered with 1 mM EGTA. (C) Examples of current responses recorded with inside-out patch of the nuclear envelope to voltage steps of 500 ms duration applied from holding potential of 0 mV. The voltage steps were of −120 to +120 mV in 20 mV increments applied sequentially every 5 s. For clarity only current responses to voltage steps (in mV) of: −100, −60, −20, +20, +60 and +100 are shown. The patch was bathed in 150 mM KCl solution and different Ca^{2+} concentrations (indicated on each panel in μM: 0, 0.16, 1.4 and 5.0) buffered with 10 mM EGTA, see Section 2. Note different current scale on upper and lower panels. At 0.16 μM Ca^{2+} single-channel current fluctuations could be resolved at +80 and +100 mV. (D) Family of NP_o-voltage relationships recorded at different Ca^{2+} concentrations (0.16, 1.4, 5.0 and 13.9 μM) in the bathing solution for the experiment shown in C. The open state probability P_o for N channels in the patch, NP_o, was calculated using the following formula: $NP_o = I/i$, where I is a steady state 'whole-patch' current at the end of a given voltage step (such as shown in C), and i is a single-channel current at the same voltage resolved by tail current analysis (such as shown in Fig. 4C,D). At each Ca^{2+} concentration the average steady state current response to a given voltage step was determined from three separate runs of the voltage protocol and was used to calculate the mean NP_o (±S.D) values. Similar results were observed with two other patches.

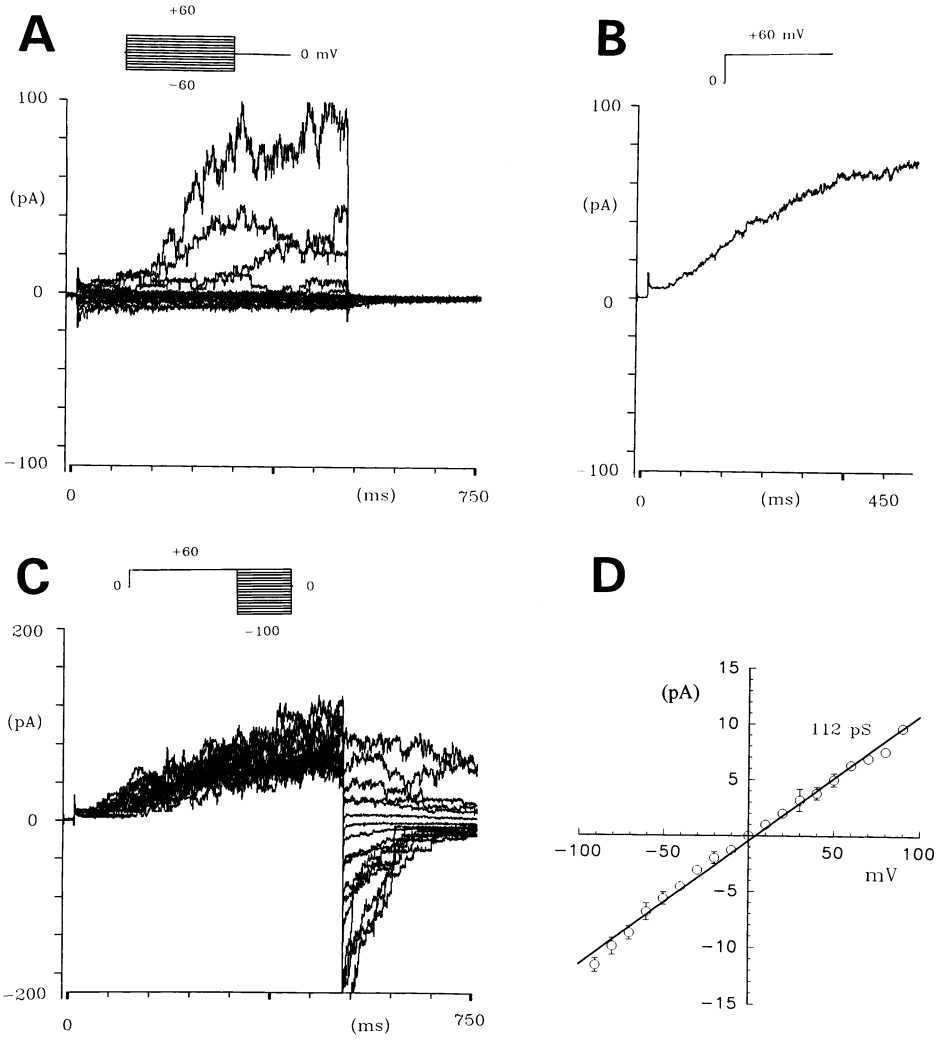

Fig. 4. Channel activation is time-dependent. (A) Current responses to a series of voltage steps of −60 to +60 mV applied in 10 mV increments from a holding potential of 0 mV (see inset for the schematic of the voltage protocol). The voltage steps were applied every 5 s and were of 500 ms duration. The experiment shown was performed with an excised outside-out patch, and bath and pipette contained the same 150 mM KCl medium with 1 mM $CaCl_2$. (B) Ensemble average of 13 individual current traces (shown in C) recorded in response to a +60 mV voltage step. Only the first 500 ms of the traces shown in C were used for averaging. (C) The same patch as in A was subjected to a 500 ms pre-pulse of +60 mV and the voltage was then stepped to different levels (between −100 and +60 mV) to record tail currents. (D) Current–voltage relation of the elementary current steps resolved in tail currents such as shown in C. The data points are means ± standard deviation (error bars are shown if greater than the symbol size) from five runs similar to that shown in C. The solid line represents the least square fit of a linear function to the data points and gives a slope conductance of 112 pS.

tential were also seen as a result of the difference in cation concentration across the membrane. In another series of experiments, the selectivity of the channel for different cations was tested. Each experiment usually started with 150 mM KCl in the pipette and in the bath. Replacing bath K^+ by 140 mM Na^+ or 150 mM Cs^+ shifted the reversal potential by $+1 \pm 3$ mV ($n=4$) and -30.5 ± 3.5 mV ($n=3$), respectively (Fig. 5B,C). Thus the channel did not discriminate between K^+ and Na^+, but showed somewhat lower permeability to Cs^+. In addition, with symmetrical 150 mM CsCl on both sides of the NE patch, the channel showed a significantly lower conductance of about 20 pS (Fig. 5C). Ca^{2+} was also found to permeate the channel. With an outside-out patch, when 150 mM KCl in the bath was replaced with 50 mM

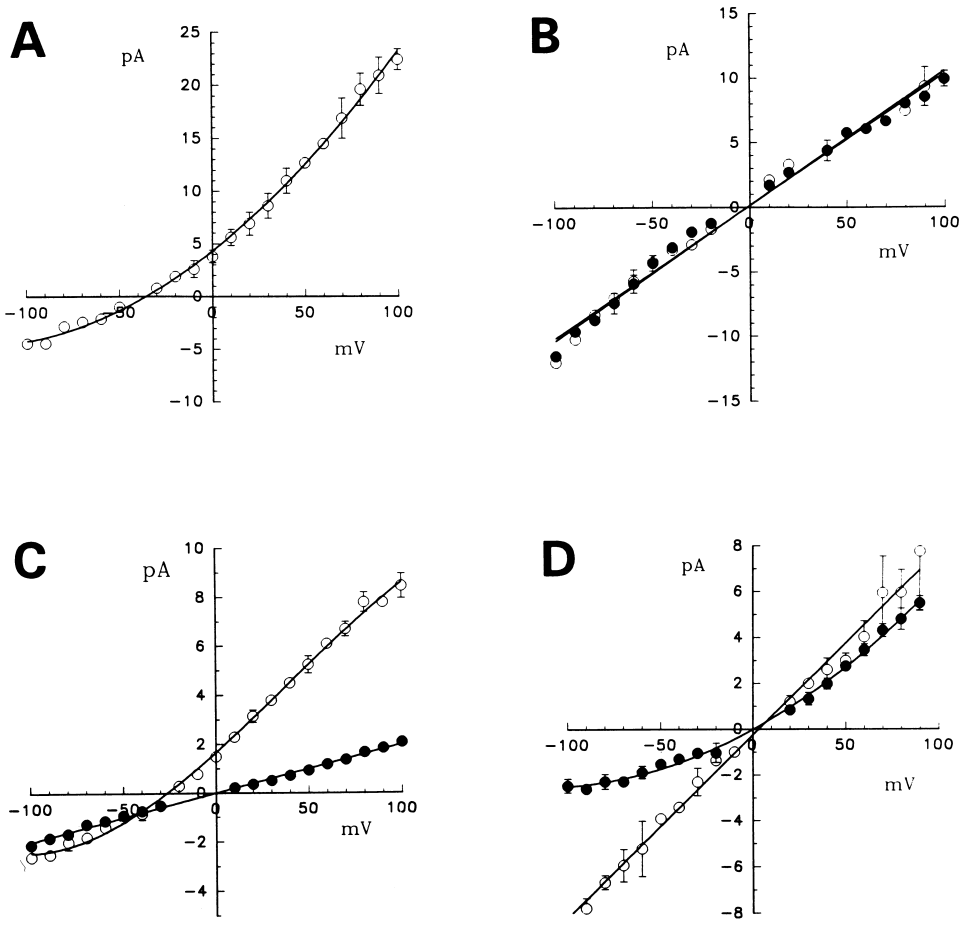

Fig. 5. Selectivity of the channel. Examples of single-channel current–voltage relations observed with excised patches of the NE in solutions of various ionic composition. (A) Inside-out patch with 50 and 300 mM KCl in pipette and bath, respectively, and with 1 mM $CaCl_2$ in both solutions. (B) Inside-out patch with symmetrical 150 mM KCl solutions on both sides (open circles) and after replacement of the bathing solution with 150 mM NaCl (filled circles). Pipette solution contained contaminating free Ca^{2+} of approximately 5 μM (see Section 2, while bath solution contained 1 mM $CaCl_2$. (C) Inside-out patch with 150 mM KCl solution in the bath and 150 mM CsCl in the pipette (open circles). The same patch in symmetrical 150 mM CsCl solution (filled circles). Both solutions contained 1 mM $CaCl_2$. (D) Outside-out patch with symmetrical 150 mM KCl solution containing 1 mM $CaCl_2$ (open circles) and after replacement of 150 mM KCl in the bath solution with 50 mM $CaCl_2$ (filled circles). The voltages shown on the figure are not corrected for liquid junction potential.

$CaCl_2$, the slope conductance was significantly reduced (to about 15 pS) at negative voltages, where the net current was mainly carried by Ca^{2+}. Under these conditions the current reversal was shifted by -2 ± 2 mV ($n = 2$) (Fig. 5D). Similar results were obtained in experiments with two inside-out patches where Ca^{2+} permeability was tested under similar ionic conditions (not shown).

3.4. Whole-nucleus recordings

In 21 whole-nucleus recordings of this study, the average nucleus capacitance was 5.1 ± 2.2 pF, while the average nucleus diameter was 15.4 ± 4.4 μm. Assuming the nucleus is an ideal sphere this gives specific capacitance of the estimated nucleus surface area, of about 0.7 ± 0.4 μF/cm^2. Fig. 6A shows whole-nucleus currents elicited by a series of voltage steps similar to that described in Fig. 4A. The pipette solution contained the standard 150 mM KCl solution with Ca^{2+} buffered with 1 mM EGTA to approximately 3 μM. As in observations with excised patches, the current is seen only at potentials positive on the nucleoplasmic side of the NE and displays

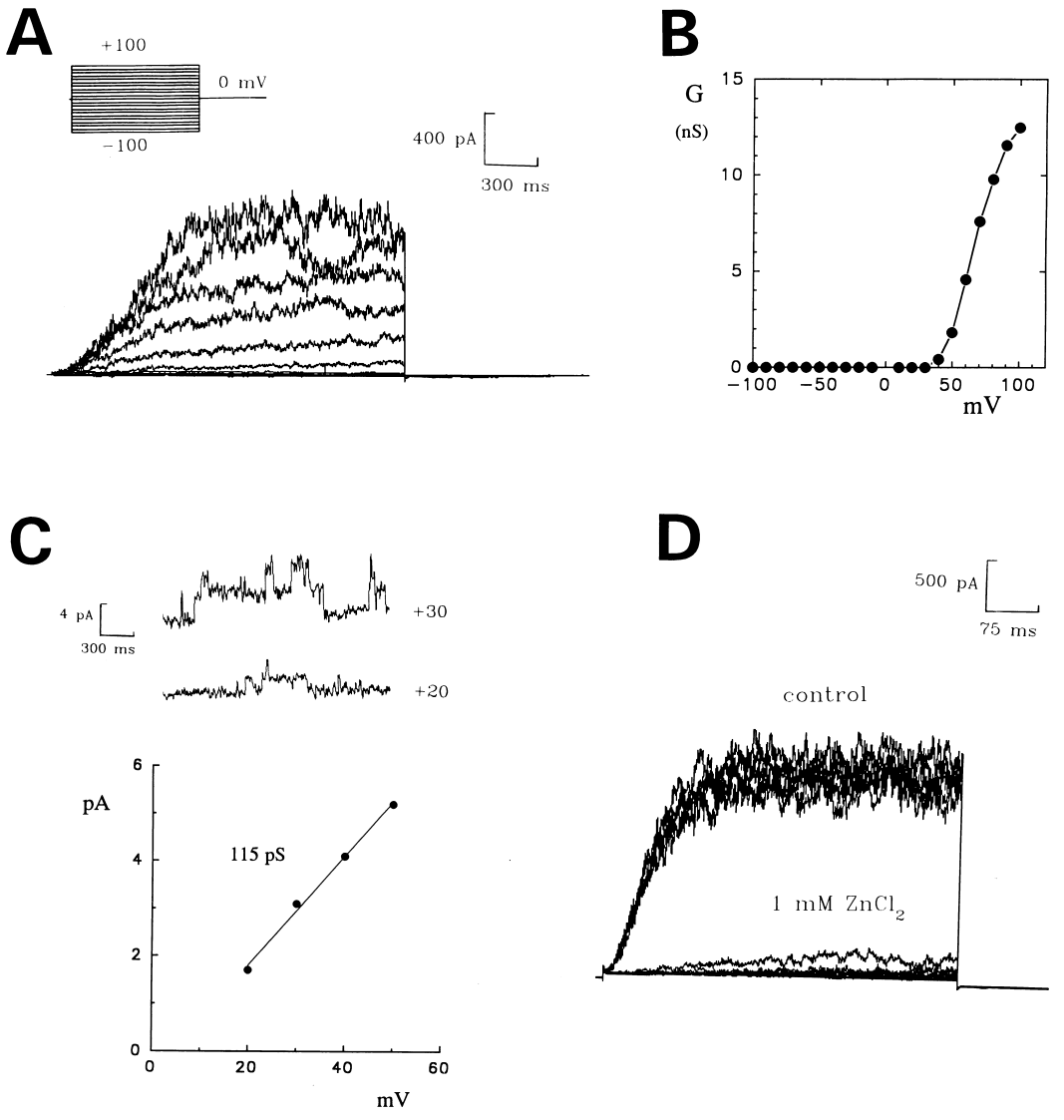

Fig. 6. Whole-nucleus currents. (A) Currents elicited by a series of voltage pulses in 10 mV increments similar to that described in Fig. 4A, except that the voltage pulses were from −100 to +100 mV and were of 2 s duration. The pipette contained the 150 mM KCl solution with 1 mM EGTA and 0.96 mM $CaCl_2$ (estimated free calcium concentration of 3 μM). The bath solution was the same as pipette except that EGTA was omitted. (B) Effect of voltage on the whole-nucleus conductance $G=I/V$ for the experiment shown in A. (C) Examples of single-channel current fluctuations resolved in whole-nucleus configuration. The current traces at +20 and +30 mV from A are shown here at higher (×100) resolution. The I–V relation of the elementary current steps gives the slope conductance of 115 pS. (D) Whole-nucleus current is blocked by Zn^{2+}. Current response to a series of 20 test pulses of +100 mV applied at 5 s intervals before and after addition (after pulse no. 6) of $ZnCl_2$ to the bath at a final concentration of 1 mM. Bath and pipette contained 150 mM KCl solution with 0.1 mM $CaCl_2$.

profound time-dependent activation during the pulse. The current in Fig. 6A seems to saturate during the 2 s voltage pulse. However, this was not always the case, and in some nuclei voltage pulses of longer duration (up to 5 s) were required to achieve saturation. We have not investigated this variability in more detail. Fig. 6B shows the voltage-dependence of the whole-nucleus conductance (G) for the experiment shown in Fig. 6A. The G values were derived from the steady-state current measured at the end of

each voltage pulse. It shows more explicitly that G is activated by voltages positive to +30 mV and saturates above +100 mV. No channel activity was seen in whole nucleus configuration when the pipette Ca^{2+} concentration was buffered with 1 mM EGTA to approximately 20 nM ($n = 3$, not shown). Thus channel activity requires micromolar Ca^{2+} concentration on nucleoplasmic side of the NE; in contrast removal of extranuclear (cytoplasmic) Ca^{2+} by chelating it with EGTA had no effect on the whole-nucleus current (not shown). Thus the current seen in whole-nucleus configuration displays voltage-, time- and Ca^{2+}-dependence similar to that observed with excised patches of the NE. In addition, the I–V relation of elementary current steps resolved in whole-nucleus recordings corresponded to the single-channel conductance observed in excised patches, (115 pS in the example shown in Fig. 6C), confirming the identity of the channel observed in all patch-clamp configurations.

Since ATP is present in millimolar concentrations in cell cytoplasm and is known to regulate activity of many transporters, we have tested its effect on our channel. Addition of 1 mM ATP to the bath had no effect on the whole-nucleus currents recorded in symmetrical 150 mM KCl and 0.1 mM $CaCl_2$ (not shown). The whole-nucleus current was blocked by Zn^{2+} (for example as shown in Fig. 6D). Here a train of test pulses of +100 mV was applied during the addition of $ZnCl_2$ to the bath at a final concentration of 1 mM. This resulted in a complete block of the current.

4. Discussion

In this study, we have applied the patch-clamp technique to examine ion channels in the nuclear envelope of the red beet. The channel described here has a conductance of about 110 pS (in symmetrical 150 mM KCl solutions), and is activated by Ca^{2+} together with positive voltages on the nucleoplasmic side of the NE. From the data shown in Fig. 3D, the NP_o-Ca^{2+} relationship can be obtained and fitted using the Hill equation. At +80 mV the fitted curve had a K_d of 2.2 μM and a Hill coefficient close to 1 indicating a first-order reaction. From the ratio of macroscopic whole-nucleus current (at +100 mV and with 3–5 μM Ca^{2+} in the pipette) to the single-channel current, it can be estimated that there are at least 200–300 channels per nucleus, depending on its size. For the average nucleus this corresponds to approximately one channel per 2 μm^2. This number represents the lower limit since the estimate is based on the assumption that $P_o = 1$ under these conditions. The channel is selective for cations over anions, but discriminates poorly between different monovalent cations. The relative permeabilities estimated from current reversal potentials using the Goldman–Hodgkin–Katz equation [27] are: $P_K \cong P_{Na} = 1$, $P_{Cs} = 0.30$ and $P_{Cl} = 0.09$. In addition, Ca^{2+} can permeate the channel. Under our experimental conditions with a 50:1 mM $CaCl_2$ gradient across NE, the current reversal potential, corrected for the liquid junction potential (see Section 2), corresponds to a Ca^{2+} permeability relative to K^+ of approximately 0.43. Despite this high permeability coefficient for Ca^{2+}, the channel conductance, at voltages that drive Ca^{2+} through the channel, was significantly reduced (to approximately 15 pS). Such a phenomenon may indicate the existence of a high-affinity binding site for Ca^{2+} within the channel pore, which slows its permeation. Despite the presence of Ca^{2+} (between a few μM to 1 mM) in the bath, the channel activity was not observed in 95% of nucleus-attached patches of intact NE, except in a few cases when the integrity of the NE could not be assured. This observation indicates that Ca^{2+} diffusion between the cytoplasm and the nucleoplasm is restricted. This was also confirmed in our preliminary Ca^{2+}-imaging experiments with isolated intact nuclei loaded with Fura-2. The basal concentrations of nucleoplasmic Ca^{2+} were 0.084 ± 0.005 μM, 0.28 ± 0.02 μM and 0.44 ± 0.03 μM with 3 μM, 100 μM and 1 mM Ca^{2+} in the bath (cytoplasmic side of the nucleus), respectively. The data are averages from 21 to 35 nuclei. Following addition of 4 μM of Ca^{2+}-ionophore A23187, nucleoplasmic Ca^{2+} increased to 0.48 ± 0.06 μM and 4.9 ± 1.4 μM for the two higher (100 μM and 1 mM) cytoplasmic Ca^{2+} concentrations respectively ($n = 10$). In nucleus-attached patch-clamp experiments performed under similar conditions, application of Ca^{2+}-ionophore resulted in activation of multilevel channel openings corresponding to conductances of 50–900 pS [19]. Further studies are required to establish if these conductances

are related to the 110 pS Ca^{2+}-activated cation channel observed with excised patch and whole-nucleus experiments.

Non-specific cation channels have been found in the nuclear envelope in other preparations: in cardiac myocytes [8], where they showed several conductance levels of 100 up to 550 pS, in avian erythrocytes [9] and in nuclei of coconut endosperm cells, with conductance levels of up to 1000 pS [28]. Their activity was independent of Ca^{2+}, and voltage had an effect only on channel inactivation. A Ca^{2+}- and Zn^{2+}-permeable channel has been identified on the inner membrane of rat liver nuclei which had a conductance of about 10 pS and its activity was independent of Ca^{2+} [29]. Recently a 166 pS, non-specific cation channel has been found in nuclei of neuronal tissue, which was neither permeable to nor gated by Ca^{2+} [30]. In contrast, the cation channel studied here shows sigmoidal time- and voltage-dependent activation and does not inactivate during prolonged depolarizing voltage steps. In addition, Ca^{2+} is required for channel activity. Thus, this is the first example of a cation channel of this type to be found in the NE. The channel activation is observed at a physiologically relevant Ca^{2+} concentrations, approximately 1 μM, and voltage close to 0 mV. Although the data on nucleus resting potential are conflicting, they were usually reported to be between 0 and −20 mV relative to cytoplasm potential, for discussion see [2]. Thus activity of our channel requires Ca^{2+} concentrations and voltages that are very likely to occur in the nucleus upon stimulation.

Ca^{2+}-activated non-selective cation channels are found in the plasma membrane of a broad range of mammalian cells [31], in the protoplast membrane of higher plant cells, e.g. in the endosperm protoplast membrane of *Haemanthus* and *Clivia* [32] as well as in the tonoplast membrane of sugar beet [33] and yeast *Sacharomyces cervisiae* [34]. These channels are all activated by cytoplasmic Ca^{2+} concentration in the order of 1 μM, but differ in single-channel conductance, pharmacological profile and voltage dependence of gating. These differences are a reflection of the diverse functions of non-selective channels in different membranes. It is obvious, that in the case of tonoplast and plasma membrane channels, their Ca^{2+} regulation can only be performed on the cytoplasmic side regardless of the Ca^{2+} source. The NE channel could potentially be regulated by Ca^{2+} from both sides: cytoplasmic and nucleoplasmic. In this context, it is interesting to note, that the channel found in the present study is not affected by changes in cytoplasmic Ca^{2+} concentration, but only by nucleoplasmic Ca^{2+}. This sidedness of Ca^{2+} regulation points to a unique role this channel may play in Ca^{2+}-dependent nuclear processes.

The functional and pharmacological properties of the channel found in the present study are different from slowly activating vacuolar (SV) non-selective cation channel in sugar beet tonoplast [33]. The SV channel was activated by cytoplasmic Ca^{2+} and hyperpolarizing voltages (vacuole inside negative), thus passing cations from cytoplasm to vacuole, while the channel found in this study is activated by nucleoplasmic Ca^{2+} and depolarizing (nucleoplasm positive) voltages. Furthermore, 2 mM cytoplasmic amiloride resulted in less than 20% inhibition of the SV channel current [35], while 2 mM amiloride applied to the nucleoplasmic side of the NE patch resulted in more than 86% inhibition of the channel activity studied here. The channel found in the present study shows approximately two-fold higher conductance, 110 pS in 150 mM KCl compared to 60–80 pS in 200 mM KCl for the SV channel, and two-fold higher selectivity for cations over anions [33]. Ca^{2+} permeability of the SV channel has not been reported; however, significant Ca^{2+} permeability was found for 150 pS non-selective cation channel of yeast (*Saccharomyces cervisiae*) tonoplast membrane. This channel was activated by cytoplasmic Ca^{2+} and depolarizing voltages (vacuole inside positive) passing cations from the vacuole to the cytoplasm [34]. Thus except for the difference in sidedness of Ca^{2+} activation, this channel seems to resemble most closely our channel of red beet NE. Similarly, the 22 pS non-selective cation channel in higher plants *Haemanthus* and *Clivia* plasma membrane was activated by cytoplasmic Ca^{2+} and depolarizing voltages (cytoplasm positive) passing ions from cytoplasm to cell exterior [32].

The nuclear envelope serves as a reservoir of Ca^{2+} and receptor operated Ca^{2+} channels such as inositol 1,4,5-trisphosphate (IP_3R) [36], inositol 1,3,4,5-tetrakisphosphate (IP_4R) [37] and ryanodine receptor (RYR) [38] have been identified on the nuclear membrane. Interestingly, IP_3R and RYR have also been located on the inner nuclear membrane [38,39], sup-

porting the concept of autonomous regulation of nuclear Ca^{2+} signals, (for a recent review on the role of Ca^{2+} in the cell nucleus see [40]). Ca^{2+}-mediated intracellular signalling is also ubiquitous in plants where Ca^{2+} mobilization involves IP_3 and cyclic ADP-ribose [41]. It is reasonable to assume, that autonomous nuclear Ca^{2+} signalling may also exist in the plants and that the channel found in this study may be part of this signalling pathway. The channel may relay information about Ca^{2+}-dependent nuclear events to the cytoplasm. It may regulate nucleoplasmic and cytoplasmic electrical potential and ion concentrations.

The simplest explanation for the fact that we have observed the same channel in all patch-clamp configurations is that the channel traverses both membranes of the NE and therefore is likely to be part of the nuclear pore complex. Our fluorescein-labeled dextran diffusion experiments indicated that in whole-nucleus configuration, the pipette solution had unrestricted connection with the nucleoplasm. Such connection may not exist between the pipette and the perinuclear space. After disrupting the patch of the NE during formation of whole-nucleus configuration, access to the perinuclear space is likely to be eliminated since outer and inner membranes are expected to fuse together and reseal, e.g. on the pipette wall. Resealing of inner and outer membranes during formation of nuclear ghosts from the *Xenopus* oocyte nuclei, resulted in preparation that behaved in a manner similar to intact, isolated nuclei [13]. Thus whole-nucleus currents that we have observed most likely represent ion fluxes between the nucleoplasm and the bath solution. Furthermore, location of the channel exclusively on the outer membrane of the NE would be inconsistent with functional properties of the channel, since it would imply regulation of the channel by perinuclear Ca^{2+}. Ca^{2+} concentration in the lumen of the NE is probably similar to that found in the lumen of the ER (100–300 μM). This concentration is approximately three orders of magnitude higher than Ca^{2+} concentrations required for dynamic regulation of channel activity (approximately 0.1–5 μM), and would result in saturating activity of the channel at all times. Estimates of the specific membrane capacitance derived from whole-nucleus experiments may help to determine whether a single or both membranes of the NE act as capacitor when subjected to a voltage step. In the absence of direct electrical coupling between the perinuclear space and nucleoplasm in whole-nucleus configuration, the two membranes would act as two spherical, approximately equal capacitors connected in series. The effective specific capacitance would be half of that for the single membrane. The mean specific capacitance of the nuclear envelope estimated from our whole-nucleus recordings is approximately 0.7 ± 0.4 $\mu F/cm^2$, while the value typically reported for biological membranes is 1 $\mu F/cm^2$ [27]. However, using patch-clamped membranes and a high resolution video microscopy to accurately estimate the membrane area, a specific, single-membrane capacitance of 0.7 $\mu F/cm^2$ was reported [42]. Recently using inflated patch-clamped cells the specific membrane capacitance was found to be 0.5 $\mu F/cm^2$ for several mammalian cells [43]. Thus, given the limited resolution of our membrane capacitance measurements, small size of our nuclei and the wide range of specific membrane capacitance reported in the literature, a definite conclusion cannot be reached. Nevertheless, the relatively low specific capacitance found in this study indicates there is little endoplasmic reticulum associated with the nucleus, as might be expected from the small amount of ER present in freshly cut storage tissue of red beet (our Fig. 2 and [26]).

In conclusion, the results presented in this report demonstrate the presence of a Ca^{2+}-regulated pathway for passive diffusion of monovalent cations and Ca^{2+} across the nuclear envelope. The channel activity is coupled to variations in nucleoplasmic Ca^{2+} concentration, therefore it may play a role in Ca^{2+}-dependent nuclear processes, such as gene transcription, protein import and apoptosis. Clearly further studies are necessary to clarify the function and physiological regulation of the channel and its localization in the NE. According to Bustamante [1], the ion channels associated with the NPC may be identifiable by their requirement for the cytoplasmic factors involved in macromolecular transport, and by their inhibition by antibodies against components of the NPC. Experiments involving fusion of vesicle fractions from the inner and outer nuclear membranes into planar lipid bilayers [5] or preparation of nuclei devoided of external membrane [29] represent alternative approaches which may help to answer some of these questions.

Acknowledgements

This work was performed in the laboratory of Dr. Ronald J. Poole, his continuous support and in-depth discussions are greatly appreciated. We also would like to thank Kathryn Hewitt, McGill EM Centre, for excellent electron microscopy study, Dr. R.A. Harris for performing calcium imaging experiments and Drs. P. Linsdell and A. Dagenais for critical reading of the manuscript.

References

[1] J.O. Bustamante, A. Liepins, J.A. Hanover, Mol. Membr. Biol. 11 (1994) 141–150.
[2] J.O. Bustamante, J. Membr. Biol. 138 (1994) 105–112.
[3] L. Stheno-Bittel, C. Perez-Terzic, A. Luckhoff, D.E. Clapham, Soc. Gen. Physiol. Ser. 51 (1996) 195–207.
[4] M. Mazzanti, News Physiol. Sci. 13 (1998) 44–50.
[5] E. Rousseau, C. Michaud, D. Lefebvre, S. Proteau, A. Decrouy, Biophys. J. 70 (1996) 703–714.
[6] S.M. Valenzuela, D.K. Martin, S.B. Port, J.M. Robbins, K. Warton, M.R. Bootcov, P.R. Schofield, T.J. Campbell, S.N. Breit, J. Biol. Chem. 272 (1997) 1275–1282.
[7] L. Tabares, M. Mazzanti, D.E. Clapham, J. Membr. Biol. 123 (1991) 49–54.
[8] J.O. Bustamante, Pfluegers Arch. 421 (1992) 473–485.
[9] A.J.M. Matzke, T.M. Weiger, M.A. Matzke, FEBS Lett. 271 (1990) 161–164.
[10] J.O. Bustamante, J. Membr. Biol. 146 (1995) 239–251.
[11] R.E. Dolmetsch, R.S. Lewis, C.C. Goodnow, J.I. Healy, Nature 386 (1997) 855–858.
[12] C. Perez-Terzic, J. Pyle, M. Jaconi, L. Stheno-Bittel, D.E. Clapham, Science 273 (1996) 1875–1877.
[13] L. Stheno-Bittel, C. Perez-Terzic, D.E. Clapham, Science 270 (1995) 1835–1838.
[14] L. Stheno-Bittel, A. Luckhoff, D.E. Clapham, Neurone 14 (1995) 163–167.
[15] O. Bachs, N. Agell, E. Carafoli, Biochim. Biophys. Acta 1113 (1992) 259–270.
[16] J.S.C. Gilchrist, M.P. Czubryt, G.N. Pierce, Mol. Cell. Biochem. 135 (1994) 79–88.
[17] A. Draguhn, G. Borner, R. Beckmann, J. Gen. Physiol. 109 (1997) 571–587.
[18] D.-O.D. Mak, J.K. Foskett, J. Biol. Chem. 269 (1994) 29375–29378.
[19] Cz Grygorczyk, R. Poole, Biophys. J. 66 (1994) A441.
[20] R. Tsien, T. Pozzan, Methods Enzymol. 172 (1989) 230–262.
[21] S.P.J. Brooks, K.B. Storey, Analyt. Biochem. 201 (1992) 119–206.
[22] O.P. Hamill, A. Marty, E. Neher, B. Sakmann, F.J. Sigworth, Pflügers Arch. 391 (1981) 85–100.
[23] E. Neher, Methods Enzymol. 207 (1992) 123–131.
[24] R. Peters, EMBO J. 3 (1984) 1831–1836.
[25] P.M. Bradley, Plant Sci. Lett. 13 (1978) 287–290.
[26] M.E. Jackman, R.F.M. Van Steveninck, Aust. J. Biol. Sci. 20 (1967) 1063–1068.
[27] B. Hille, Ionic Channels of Excitable Membranes, 2nd edn., Sinauer, Sunderland, MA, 1991.
[28] A.J.M. Matzke, C. Behensky, T. Weiger, M.A. Matzke, FEBS Lett. 302 (1992) 81–85.
[29] A.S. Longin, P. Mezin, A. Favier, J. Verdetti, Biochem. Biophys. Res. Commun. 235 (1997) 236–241.
[30] A. Draghun, G. Borner, R. Beckmann, K. Buchner, U. Heinemann, F. Hucho, J. Membr. Biol. 158 (1997) 159–166.
[31] L.D. Partridge, D. Swandulla, Trends Neurosci. 11 (1988) 69–72.
[32] H. Stoeckel, K. Takeda, Proc. R. Soc. Lond. Ser. B. 237 (1989) 213–231.
[33] R. Hedrich, E. Neher, Nature 329 (1987) 833–836.
[34] A. Bertl, C.L. Slayman, J. Exp. Biol. 172 (1992) 271–287.
[35] R. Hedrich, A. Kurkdjian, EMBO J. 12 (1988) 3661–3666.
[36] A.N. Malviya, P. Rouge, G. Vincendon, Proc. Natl. Acad. Sci. USA 87 (1990) 9270–9274.
[37] P. Köppler, N. Matter, A.N. Malviya, J. Biol. Chem. 268 (1993) 26248–26252.
[38] O.V. Gerasimenko, J.V. Gerasimenko, A.V. Tepikin, O.H. Petersen, Cell 80 (1995) 439–444.
[39] J.P. Humbert, N. Matter, J.C. Artault, P. Köppler, A.N. Malviya, J. Biol. Chem. 271 (1996) 478–485.
[40] A.N. Malviya, P.J. Rogue, Cell 92 (1998) 17–23.
[41] G.J. Allen, S.R. Muir, D. Sanders, Science 268 (1995) 735–737.
[42] M. Sokabe, F. Sachs, Z.Q. Jing, Biophys. J. 59 (1991) 722–728.
[43] C. Solsona, B. Innocenti, J.M. Fernandez, Biophys. J. 74 (1998) 1061–1073.